http://dx.doi.org/10.5012/bkcs.2012.33.6.1983

Fluorescently Labeled Nanoparticles Enable the Detection of Stem Cell-Derived Hepatocytes

Youngeun Ha, Jin-sup Shin, Dong Yun Lee, and Taiyoun Rhim†,*

Department of Bioengineering, College of Engineering, Hanyang University, Seoul 133-791, Korea
†Institute for Bioengineering and Biopharmaceutical Research, Hanyang University, Seoul 133-791, Korea
**E-mail: rhim@hanyang.ac.kr*
Received March 9, 2012, Accepted March 19, 2012

Stem cell transplantation is emerging as a possible new treatment for liver cirrhosis, and recent animal studies have documented the benefits of stem cell therapy in a hepatic fibrosis model. However, the underlying mechanism of stem cell therapy is still unclear. Among the proposed mechanisms, the cell replacement mechanism is the oldest and most important, in which permanently damaged tissue can be replaced by normal tissue to restore function. In the present study, Cy5.5-labeled superparamagnetic iron oxide (SPIO) was used to label human mesenchymal stem cells. The uptake of fluorescently labeled nanoparticles enabled the detection and monitoring of the transplanted stem cells; therefore, we confirmed the direct incorporation and differentiation of SPIO into the hepatocyte-like transplanted stem cells by detecting human tyrosine aminotransferase (TAT), well-known enzymatic marker for hepatocyte-specific differentiation.

Key Words : Liver cirrhosis, Mesenchymal stem cell transplantation, Fluorescently labeled nanoparticles, Hepatocyte-specific differentiation

Introduction

Hepatic fibrosis is characterized by the excessive deposition of extracellular matrix, or scar tissue, in response to acute or chronic liver injury.[1] Fibrosis is a reversible wound healing process characterized by the accumulation of extracellular matrix with thin fibrils and no tuberculation.[2] Therefore, complete recovery follows the removal of the causal factor that induces the tissue damage. However, chronically repetitive mechanisms of liver fibrosis may lead to hepatic cirrhosis, which was the tenth leading cause of death for men in the United States in 2001 and the 12th for women, killing about 27,000 people each year.[3] In the process of repeated injury and repair, normal liver parenchyma is gradually replaces with fibrotic tissue; therefore, it is characterized by the excessive deposition of extracellular matrix consisting of collagen and a relative lack of parenchymal cells in the liver. The rearranged structure by the scar tissue impairs blood flow in the liver tissue. The replacement of normal liver with scar tissue also causes an irreversible decrease in liver function through the loss of normal liver tissue.[4]

Fibrosis creates permanent scar tissue.[5] For this reason, liver cirrhosis is a disease that is difficult to treat and has a substantial morbidity and mortality rate.[6] In fact, treatment options for liver cirrhosis are very limited.[2] To date, there is no treatment available to reverse liver cirrhosis. The existing treatments for liver cirrhosis aim to stop the progress of cirrhosis and to reduce disabling or life-threatening treatment complications.

Liver transplantation is considered a last option for the recovery of non-functioning liver.[7] However, liver transplantation has many problems such as the limitation of available donor livers, surgical complications, and rejection. With advancements in stem cell research and development, stem cell therapy has recently become a viable alternative to organ transplantation.[8] Recent studies using bone marrow-derived mesenchymal stromal cell-based therapy have shown promising results in animal experiments.[9-11] Systemic administration of mesenchymal stem cells (MSCs) reduced extra cellular matrix protein deposition,[12] and the MSCs were shown to regenerate hepatocytes in injured liver.[13] More recently, Kamada *et al.* reported that adipose tissue-derived stromal cells (ADSCs) contributed to the regression of liver function and fibrosis in CCl_4-induced mouse liver fibrosis.[14] However, some research has insisted that the contribution of BM-derived hepatocytes to the replacement of injured livers may be very low except for in certain limited experimental conditions.[15-17]

In this study, we attempted to show the direct differentiation of transferred MSCs into hepatocytes using superparamagnetic iron oxide (SPIO) particles for magnetic labeling of MSCs in order to better understand the exact role of MSC transplantation in liver cirrhosis.

Materials and Methods

Human Mesenchymal Stem Cells. Bone marrow-derived human mesenchymal stem cells (MSCs) were purchased from Lonza and cultured in high glucose Dulbecco's modified Eagle's medium (DMEM) containing 10% fetal bovine serum, 100 units/mL penicillin, and 0.1 mg/mL streptomycin at 37 °C in a 5% CO_2 atmosphere.

Animal Model. Female C57BL/6J mice (5 weeks old)

were purchased from Japan SLC, Inc. (Shizuoka, Japan) and randomly divided into a cirrhotic group (n = 20) and a normal control group (n = 10). In the cirrhotic group, CCl_4 (4:1 olive oil) at a dose of 0.1 mL/100 g body weight was injected into the peritoneum twice a week. After 5 weeks, the mice in the cirrhotic group were randomly divided into two groups: a control cirrhotic group (n = 10) and a cell transplantation group (n = 10). Mice in the stem cell transplantation group were injected with hMSCs (human mesenchymal stem cells) via the tail vein under anesthesia at 5 weeks and 7 weeks. All C57BL/6J mice were weighed once a week. Mice of all groups were sacrificed at 8 weeks. All care and experimental procedures for the mice were performed under the guidelines of Hanyang University Policy for Experiments in Animals, and all protocols were approved by the IACUC of the Hanyang University.

Preparation of Cy5.5-conjugated UFH-SPIO. Superparamagnetic iron oxide (SPIO) nanoparticles were prepared as in previous works.[18,19] Briefly, $FeCl_2 \cdot 4H_2O$ (185 mg; Sigma, St. Louis, MO, USA) and $FeCl_3 \cdot 6H_2O$ (500 mg; Sigma) were dissolved in deoxygenated distilled water (30 mL) for 30 min. Then, an ammonium hydroxide solution (NH_4OH, 7.5 mL) was added under N_2 gas while stirring for 30 min at room temperature. An external magnetic field (M_{ext}) was then applied to the solution to rinse the formed SPIO nanoparticles with distilled water. In the SPIO dispersed solution, 250 mg/20 mL distilled water of UFH (Nanjing King-Friend Biochemical Pharmaceutical Co., Ltd., Nanjing, China) was added and stirred for 2 h. The final product was washed with fresh distilled water and then sonicated using a VCX-500 Ultrasonic Processor (60 min at 200W; Sonics & Materials, Inc., Newtown, CT). After sonication, M_{ext} was applied again for 6 h to precipitate the aggregated nanoparticles, and the supernatant (dispersed nanoparticles) was then centrifuged three times at 4000 rpm for 10 min and heated at 80 °C for 1 h to obtain nanoparticle stabilization. The final UFH-SPIO nanoparticles were stored at 4 °C until use. Separately, Cy5.5-conjugated UFH-SPIO nanoparticles were prepared via crosslinking the primary amine group of UFH. To this end, 1 mL of UFH SPIO (pH 8.5 adjusted with 0.1 M sodium bicarbonate) was added to 1 mg of Cy5.5 NHS ester (Lumiprobe Corp., Hallandale Beach, FL, USA) and stirred for 6 h at room temperature. M_{ext} was then applied to the solution to rinse the Cy5.5-conjugated UFH-SPIO nanoparticles with distilled water. The final product was stored in the dark.

Histology. For histological analysis, half of the specimens were fixed in 10% (v/v) buffered formaldehyde, dehydrated with a series of graded ethanol, and embedded in paraffin. Specimens were sliced into 4-μm-thick sections and stained with H&E or Masson's trichrome to evaluate collagen production. Prussian blue staining was performed to detect SPIO molecules using equal volumes of 1 N HCl and 10% potassium ferrocyanide (30 min) and counterstained with 1% neutral red (2 min). Microscopic examination was performed and photographed under a regular light microscope.

Fibrosis volume was quantified with Masson's trichrome staining as the area stained positive for collagen. Fibrotic and non-fibrotic areas were calculated by integrating ten fibrosis section volumes, where fibrosis volume was defined as (blue area/total area) × (weight of each section/total weight of 10 sections) × 100%.

Near-infrared Liver Imaging. To obtain *ex vivo* fluorescence images, we used hMSCs that had accumulated Cy5.5-labeled SPIO. At one week post-injection, mice were sacrificed, the liver was dissected, and fluorescence images were obtained. Fluorescence imaging was performed using a Kodak Image Station 4000MM (Digital Imaging System, New Haven, CT) equipped with a special C-mount lens and a Cyanine 5.5 emission filter. The near-infrared fluorescence images were acquired with a 1 s exposure time.

Nested RT-PCR (reverse transcription-PCR). Total RNA was isolated from liver tissue using TRIzol reagent (Invitrogen, Carlsbad, CA, USA) according to the manufacturer's instructions. The cDNA was prepared using a Superscript II kit (Invitrogen) according to the manufacturer's instructions. The human tyrosine aminotransferase (TAT) cDNA was amplified by PCR (30 sec 94 °C, 30 sec at 55 °C, and 45 sec at 72 °C for 35 cycles) using the 1hTATf and 1hTATr primers d(TGTGTCCCCATCTTAGCTGAT) and d(AATGGTACAGGGTCCCAAAATG), respectively, which amplify a 246 bp sequence, followed by a second PCR with the 2hTATf and 2hTATr d(AACCACTGGCCACCCTCAGCAC) and d(AGCTTCACCAGCCCATCTCGGA) nested primers, respectively, which amplify a 154-bp sequence. The primers used for PCR amplifying β-actin RNA were d(GTCTTCACCACCATGGAG) and d(TCATCATATTTGGCAGGTTT).

Western Blot. Protein extracts were obtained from liver tissue and lysed by sonication in PBS containing 1 mM PMSF. Proteins were resolved by 12.5% SDS-PAGE and transferred to a PVDF membrane (Millipore, Milan, Italy). The membrane was blocked for 1 hr in a 5% skim milk solution and then incubated with polyclonal rabbit anti-mouse collagen type I antibody (1:500 dilution) (Millipore, Milan, Italy) for 2 hr at room temperature. The unbound primary antibodies were removed with one 15 min and two 5 min washes in PBS containing 0.1% (v/v) Nonidet P-40. Then, the membrane was incubated with horseradish peroxidase-conjugated goat anti-mouse IgG secondary antibody (Ab Frontier, Seoul, Korea) for 2 hr at room temperature. The target protein was detected by ECL solution (Amersham Biosciences, Cleveland, OH, USA) using X-ray film.

Statistical Analysis. All quantitative data are expressed as mean ± standard deviation. Statistical analysis was performed with one-way analysis of variance (ANOVA) using SPSS software (SPSS Inc., Chicago, IL). A value of $p < 0.05$ was considered statistically significant.

Results

Successful Delivery of hMSCs. To trace hMSCs, the cells were labeled with SPIO and then intravenously injected into the liver cirrhosis mouse model. Before injection, uptake of

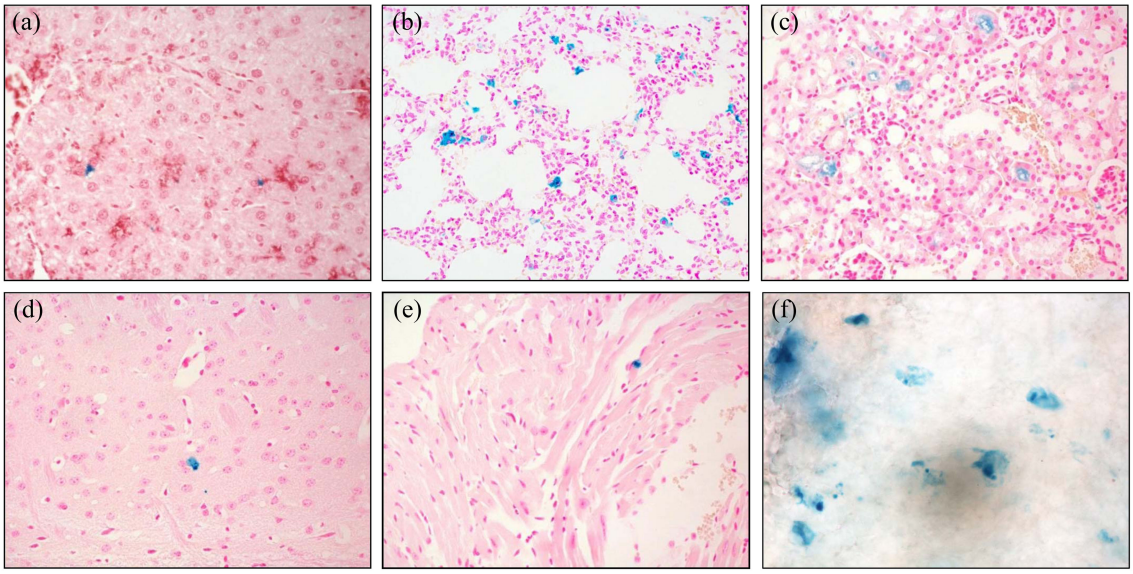

Figure 1. Histologic findings of SPIO-labeled hMSCs in the mouse liver (a), lung (b), kidney (c), brain (d), heart (e), and bone marrow (F) 2 weeks after transplantation.

SPIO was confirmed to be positive for Prussian blue staining (data not shown). After 2 weeks, mice were sacrificed, and all tissues including the bone marrow were collected and examined histologically. As shown in Figure 1, all the tissues that we examined including the liver, lung, kidney, heart, and brain had positively-stained cells. Tail vein-injected stem cells were mainly detected in the lungs and bone marrow (Panels B and F). In contrast, labeled cells were hardly detected in liver, brain, and heart tissues, in which less than 10% of the tissue sections contained positively stained cells.

Improvement of Hepatic Function and Morphology. Macroscopically, the CCl_4-treated mice livers appeared pale and nodular on the external surface compared to normal

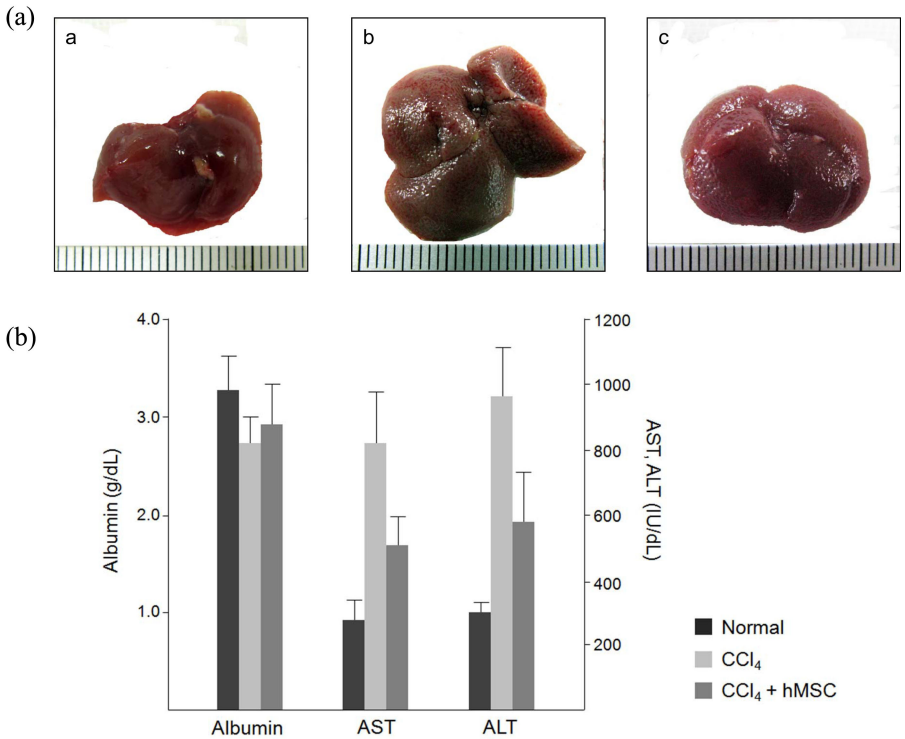

Figure 2. hMSC treatment improved hepatic function and morphology. Representative macroscopic appearance of mouse livers (a). Fibrosis bands were seen in the disease group ((a)b), whereas the intensity of the fibrosis band was reduced in the hMSC transplanted group ((a)c). Restoration of hepatic function was tested using biochemical markers of liver function (b). The bars indicate standard deviation.

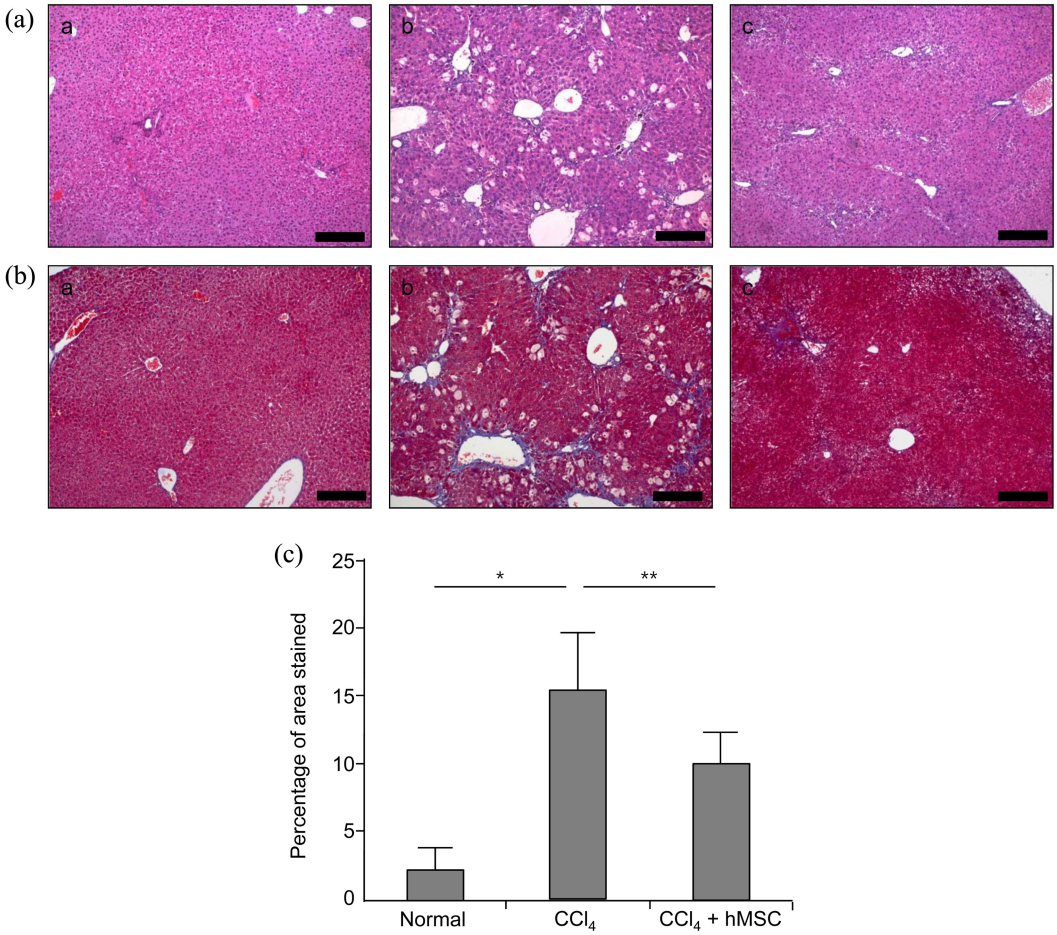

Figure 3. Histopathological examination revealed that hMSC transplantation reduced hepatic fibrosis. Hematoxylin and Eosin stain (a). Masson's trichrome stain for extracellular matrix protein (b). Scale bar = 200 mm. Quantitative analysis of fibrosis (c). Fibrotic areas were quantified by an image analysis program. *$p < 0.0001$, ** $p < 0.05$.

the internal structure of the liver, and hepatic cells multiply to form regeneration nodules separated by white scar tissue, resulting in an irregular cirrhotic liver surface. Repeated injection of CCl_4 induced liver fibrosis; however, the administration of hMSCs suppressed the CCl_4-induced macroscopic changes (Fig. 2(a)c).

Functionally, transplantation of hMSCs could upregulate the decrease of albumin in CCl_4-treated mice serum (Fig. 2(b)). Albumin is exclusively produced in the liver, so albumin serum level may reflect changes in liver function. The administration of hMSCs also downregulated the increases in alanine transaminase (ALT) and alanine transferase (AST) in CCl_4-treated mice serum (Fig. 2(b)). These findings indicate that hMSC transplantation can restore liver function.

Decreased Fibrosis After hMSC Injection. After 8 weeks of CCl_4 challenge, liver samples were stained with H&E and Masson's trichrome to evaluate histopathologic changes and tissue fibrosis. The degree of liver fibrosis was evaluated histologically using Masson's trichrome staining. Fibrosis developed in the livers of CCl_4-treated mice. However, 2 weeks after hMSC treatment, the degree of inflammation and collagen deposition (Masson's stained) decreased (Figs.

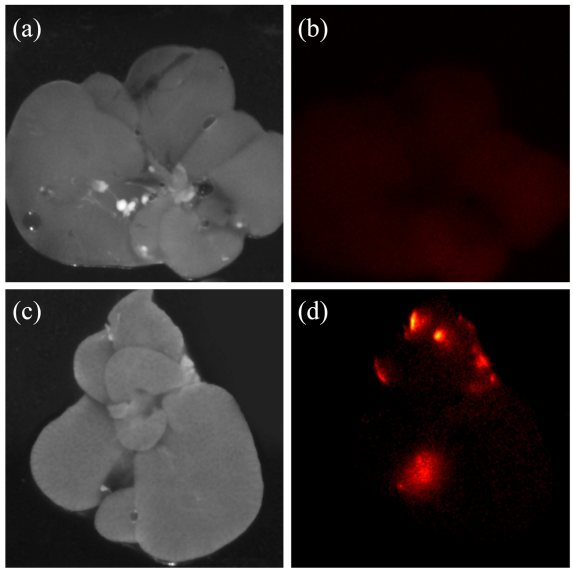

Figure 4. *Ex vivo* color-coded map images of livers excised from mice transplanted with Cy5.5-labeled SPIO harboring hMSCs. Fluorescence was detected in the livers of labeled stem cell transplanted mice. Fluorescent area was excised for RNA preparation.

(a)

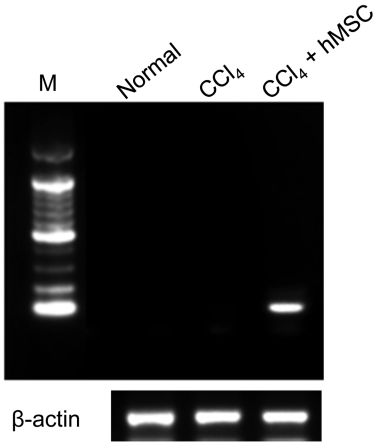

(b)

```
RT-PCR: ctggctggttcctggctggaggttgggctggatcctcattcatgaccgaagagacatttttggcaatgagatccgagatgggctggtgaagct
        ||||||||||||||||||||||||||||||||||||||||||||||||||||||||||||||||||||||||||||||||||||||||||||||||
Human : ctggctggttcctggctggaggttgggctggatcctcattcatgaccgaagagacatttttggcaatgagatccgagatgggctggtgaagct 100.0%
        |||||||||||||||||||||||| |||||||||||| || ||||| |||||||||||||||||||||||||||| || || ||||||||||||||
Mouse : ctggctggttcctggctggaggctgggctggatccttatccatgatcgaagagacatttttggcaatgagattcgggacgggctggtgaagct 92.4%
```

Figure 5. Detection of differentiated hMSCs in mice livers. TAT (tyrosine aminotransferase) expression was detected in hMSC transplanted mouse liver (a). Amplified cDNA sequence was determined and compared with mouse (NM_146214) and human TAT (NM_000353) cDNA sequences (b). As illustrated above, this comparison reveals that the amplified gene is human TAT.

3(b) and (c)). For quantification of histological data, we examined the tissue slides from all liver sections, and the results are expressed as percentages. As shown in Figure 3(d), the area occupied by blue-stained collagen was decreased significantly by hMSC transplantation (15.4% *vs.* 10.1%, $p = 0.002$).

Detection of Differentiated hMSCs in Mouse Liver. To examine whether transplanted hMSCs developed into functionally active liver cells, we conducted RT-PCR. First, we excised the Cy5.5-labeled liver tissue to enrich the RNA from transplanted cells. Transplanted hMSCs emitted red fluorescence because they contained the Cy5.5-conjugated UFH-SPIO nanoparticles (Fig. 4). Second, total RNAs were extracted from excised tissue and reverse transcribed with oligo dT primers. As shown in Figure 5, the gene expression of human tyrosine aminotransferase, a marker of adult hepatocytes, was found only in hMSC transplanted mouse livers according to nested RT-PCR. The amplified PCR products showed 100% sequence homology to the human TAT. In addition, the primers that we used in RT-PCR were specific to different exons within the human TAT gene. These results suggest that transplanted hMSCs directly differentiate into functional hepatocytes.

Discussion

Hepatic cirrhosis is generally characterized by the irreversible remodeling of liver tissue; therefore, treatments usually focus on preventing progression and complications. Recently, numerous reports have published on the therapeutic effects of stem cell transplantation on liver cirrhosis.[20-26] These studies used various types of adult and embryonic stem cells to restore liver function and morphology. In addition, they attempted to show the direct incorporation of transplanted stem cells on target tissue. Zhan *et al.* labeled hematopoietic stem cells with the fluorophore PKH26-GL,[22] and Ju *et al.* used magnetically labeled green fluorescent protein (GFP) to indicate mesenchymal stem cells.[25] Abdel Aziz *et al.* showed the incorporation of stem cells in target tissue using Y-chromosome gene (*sry*)-specific PCR.[23] However, no group has shown direct evidence of *in vivo* differentiation into functional hepatocyte-like cells.

In the present study, we demonstrate that transplanted hMSCs incorporated and differentiated into hepatocyte-like cells in injured liver tissue using Cy5.5-labeled SPIO particles. To provide direct evidence of transplanted stem cell incorporation and differentiation, we choose human mesenchymal stem cells instead of male mouse stem cells. When male origin stem cells are used, the incorporated cells can be identified using a Y-chromosome-specific gene probe. However, this method does not tell us whether the transplanted cells differentiated into functionally active cells. When we used a kind of xenotransplantation in this study, we could detect functionally differentiated cells using sequence differences between the human and mouse genes. In this report, we analyzed tyrosine aminotransferase gene expression and its sequence. Tyrosine aminotransferase (TAT) is a well-known enzymatic marker for hepatocyte-specific differentiation.[27]

Frankly, we failed to amplify the human TAT gene even when we used nested RT-PCR from cDNA made from whole bovine liver. As in Figure 1, SPIO-containing hMSCs were seldom detected in liver tissue. We used Cy5.5-labeled heparin to overcome the extremely small amount of target sample, which was coated in SPIO molecules as a visual marker. Therefore, the hMSCs were stably labeled with fluorescence. In this case, the total RNA was purified from the fluorescently labeled tissue area to enrich the target

RNA.

In conclusion, the underlying mechanism of stem cell therapy is still unclear in most diseases. We do not think that the therapeutic effects can be explained by a single factor. However, it is still important to show that the transplanted stem cells were directly incorporated and differentiated into functional progeny. To this end, fluorescently labeled SPIO is quite useful to label and follow transplanted stem cells.

Acknowledgments. This work was supported by the research fund of Hanyang University Institute of Aging Society in 2010.

References

1. Friedman, S. L. *J. Gastroenterol.* **1997**, *32*(3), 424.
2. Safadi, R.; Friedman, S. L. *MedGenMed.* **2002**, *4*(3), 27.
3. Anderson, R. N.; Smith, B. L. *National Vital Statistics System* **2003**, Vol 52.
4. Purohit, D. A. *Hepatology* **2006**, *43*, 872.
5. Galicia-Moreno, M.; Rodríguez-Rivera, A.; Reyes-Gordillo, K.; Segovia, J.; Shibayama, M.; Tsutsumi, V.; Vergara, P.; Moreno, M. G.; Muriel, P. *Eur. J. Gastroenterol. Hepatol*. **2009**, *21*(8), 908.
6. Hattori, S.; Dhar, D. K.; Hara, N.; Tonomoto, Y.; Onoda, T.; Ono, T.; Yamanoi, A.; Tachibana, M.; Tsuchiya, M.; Nagasue, N. *Lab. Invest*. **2007**, *87*(6), 591.
7. Selberg, O.; Böttcher, J.; Tusch, G.; Pichlmayr, R.; Henkel, E.; Müller, M. J. *Hepatology* **1997**, *25*(3), 652.
8. Dan, Y. Y.; Yeoh, G. C. *Gastroenterol. Hepatol*. **2008**, *23*(5), 687.
9. Lee, K. D.; Kuo, T. K.; Whang-Peng, J.; Chung, Y. F.; Lin, C. T.; Chou, S. H.; Chen, J. R.; Chen, Y. P.; Lee, O. K. *Hepatology* **2004**, *40*, 1275.
10. Saji, Y.; Tamura, S.; Yoshida, Y.; Kiso, S.; Iizuka, A. S.; Matsumoto, H.; Kawasaki, T.; Kamada, Y.; Matsuzawa, Y.; Shinomura, Y. *J. Hepatol.* **2004**, *41*, 545.
11. Sato, Y.; Araki, H.; Kato, J.; Nakamura, K.; Kawano, Y.; Kobune, M.; Sato, T.; Miyanishi, K.; Takayama, T.; Takahashi, M.; Takimoto, R.; Iyama, S.; Matsunaga, T.; Ohtani, S.; Matsuura, A.; Hamada, H.; Niitsu, Y. *Blood* **2005**, *106*, 756.
12. Bahk, J. Y.; Piao, Z.; Jung, J. H.; Han, H. In *Stem Cells in Clinic and Research*; Intech: 2011.
13. Sharma, A. D.; Cantz, T.; Richter, R.; Eckert, K.; Henschler, R.; Wilkens, L.; Jochheim-Richter, A.; Arseniev, L.; Ott, M. *Am. J. Pathol*. **2005**, *167*(2), 555.
14. Kamada, Y.; Yoshida, Y.; Saji, Y.; Fukushima, J.; Tamura, S.; Kiso, S.; Hayashi, N. *Am. J. Physiol. Gastrointest. Liver Physiol*. **2009**, *296*(2), G157.
15. Kanazawa, Y.; Verma, I. M. *Proc. Natl. Acad. Sci.* USA **2003**, *100*, 11850.
16. Menthena, A.; Deb, N.; Oertel, M.; Grozdanov, P. N.; Sandhu, J.; Shah, S.; Guha, C.; Shafritz, D. A.; Dabeva, M. D. *Stem Cells* **2004**, *22*(6), 1049.
17. Wagers, A. J.; Weissman, I. L. *Cell* **2004**, *116*(5), 639.
18. Lee, D. Y. *Macromol. Res*. **2011**, *19*(8), 843.
19. Jung, M. J.; Lee, S. S.; Hwang, Y. H.; Jung, H. S.; Hwang, J. W.; Kim, M. J.; Yoon, S.; Lee, D. Y. *Biomaterials* **2011**, *32*, 9391.
20. Fang, B.; Shi, M.; Liao, L.; Yang, S.; Liu, Y.; Zhao, R. C. *Transplantation* **2004**, *78*(1), 83.
21. Zhao, D. C.; Lei, J. X.; Chen, R.; Yu, W. H.; Zhang, X. M.; Li, S. N.; Xiang, P. *World J. Gastroenterol*. **2005**, *11*(22), 3431.
22. Zhan, Y.; Wang, Y.; Wei, L.; Chen, H.; Cong, X.; Fei, R.; Gao, Y.; Liu, F. *Transplant. Proc*. **2006**, *38*(9), 3082.
23. Abdel Aziz, M. T.; Atta, H. M.; Mahfouz, S.; Fouad, H. H.; Roshdy, N. K.; Ahmed, H. H.; Rashed, L. A.; Sabry, D.; Hassouna, A. A.; Hasan, N. M. *Clin. Biochem*. **2007**, *40*(12), 893.
24. Jung, K. H.; Shin, H. P.; Lee, S.; Lim, Y. J.; Hwang, S. H.; Han, H.; Park, H. K.; Chung, J. H.; Yim, S. V. *Liver Int.* **2009**, *29*(6), 898.
25. Ju, S.; Teng, G. J.; Lu, H.; Jin, J.; Zhang, Y.; Zhang, A.; Ni, Y. *Invest. Radiol*. **2010**, *45*(10), 625.
26. Cho, K. A.; Lim, G. W.; Joo, S. Y.; Woo, S. Y.; Seoh, J. Y.; Cho, S. J.; Han, H. S.; Ryu, K. H. *Liver Int*. **2011**, *31*(7), 932.
27. Coleman, W. B.; Smith, G. J.; Grisham, J. W. *J. Cell Physiol.* **1994**, *161*, 463.